Int. J. Electrochem. Sci., 8 **(2013)** 1103 - 1116

International Journal of
ELECTROCHEMICAL
SCIENCE
www.electrochemsci.org

Effect of Equal-Channel Angular Pressing Passes on the Corrosion Behavior of 1050 Aluminum Alloy in Natural Seawater

El-Sayed M. Sherif[1], *Mahmoud S. Soliman*[2,*], *Ehab A. El-Danaf*[2], *A. A. Almajid*[1,2]

[1] Center of Excellence for Research in Engineering Materials (CEREM), Advanced Manufacturing Institute, College of Engineering, King Saud University, P. O. Box 800, Al-Riyadh 11421, Saudi Arabia
[2] Department of Mechanical Engineering, College of Engineering, King Saud University, P.O. Box 800, Al-Riyadh 11421, Saudi Arabia
[*]E-mail: solimanm@ksu.edu.sa

Received: 21 November 2012 / *Accepted:* 18 December 2012 / *Published:* 1 January 2013

In this work, the 1050 aluminum alloy (AA 1050) was processed by using equal-channel angular pressing (ECAP) technique for different number of passes namely; 0, 4, 6, 8, 12 and 16 passes. The effect of ECAP passes on the corrosion behavior of AA 1050 in Arabian Gulf seawater (AGS) has been investigated. Cyclic potentiodynamic polarization (CPP), chronoamperometric current-time (CT), and electrochemical impedance spectroscopy (EIS) measurements for AA 1050 after 20 min and 10 days immersion in the AGS solutions were carried out at room temperature. Polarization curves and chronoamperometric experiments at –0.63 V vs. Ag/AgCl indicated that the ECAPed AA 1050 shows lower corrosion current density, higher corrosion resistance and less corrosion rate compared to the unprocessed (annealed) alloy and the best performance for the alloy was obtained after 4 passes. EIS spectra confirmed the data obtained by CPP and CT measurements that the ECAPed AA 1050 alloy showed a lower corrosion rate and higher surface and polarization resistances; this effect changes in the order of 4 > 6 > 8 > 12 >16 > 0 passes. This effect increases also with increasing the immersion time of AA 1050 in the AGS solution from 20 min to 10 days.

Keywords: equal-channel angular pressing (ECAP); AA 1050; Arabian Gulf seawater; corrosion passivation; cyclic polarization; electrochemical impedance spectroscopy

1. INTRODUCTION

Aluminum is one of the most versatile and sustainable materials for our dynamic global economy. Its alloys have been generally used in manufacturing automobile and aircraft components, household appliances, containers, and electronic devices [1-9]. This is due to their excellent

combination of properties, e.g. good corrosion resistance, excellent thermal conductivity, high strength to weight ratio, easy to deform, and high ductility.

AA 1050 is a popular grade of aluminum for general sheet metal work where moderate strength is required. It is known for its excellent corrosion resistance, high ductility and highly reflective finish. The alloy is typically used for chemical process plant equipment, food industry containers, pyrotechnic powder, architectural flashings, lamp reflectors, cable sheathing. The excellent corrosion resistance of this alloy arises from its ability to form a natural oxide film on its surface in a wide variety of media [6–10]. This oxide film can readily undergo corrosion reactions in corrosive environments, especially those containing chloride ions such as sea water [6–13].

It has been reported [10-23] that the protection of aluminum against corrosion in aggressive media can achieved either by adding other alloying elements and/or by decreasing the corrosivity of its surrounding environments. The use of an organic or inorganic corrosion inhibitor is one of the most useful ways in decreasing the aggressiveness action of the environment on metals and alloys corrosion [10-21]. Protective coatings applied on surfaces of materials have also been reported [22, 23] to be used to eliminate the corrosivity of an environment.

Equal channel angle pressing (ECAP) is a processing procedure whereby an intense plastic strain is imposed by pressing a sample in a special die [24]. The ECAP procedures lead to substantial grain refinement so that the grains are reduced to the submicrometer or even the nanometer range [25,26]. The method is considered as one of the very useful techniques for producing ultra-fine microstructures of Al-based alloys with significantly improved mechanical properties and higher corrosion resistance [3,27-30]. Moreover, ECAP have been utilized not only to obtain ultrafine-grained materials but also to produce extraordinary mechanical and physical properties without remarkably changing the geometry of a bulk material. Materials processed with ECAP become superior to that of conventional coarse-grained materials [24, 31-36].

In our previous work [3], the effect of 1 to 4 ECAP passes on the corrosion passivation of the processed AA 1050 in Arabian Gulf water was reported. It was found that the corrosion rate decreases and resistance for uniform and pitting attacks increases with increasing the number of passes and the best performance was obtained for the ECAPed AA 1050 alloy after 4 passes. In the present study, the effect of increasing ECAP pass number up to 16 on the corrosion of AA 1050 in Arabian Gulf seawater is investigated. The work was carried out by using cyclic potentiodynamic polarization, chronoamperometric current-time variations, and electrochemical impedance spectroscopy.

2. EXPERIMENTAL

2.1. Materials and electrochemical cell

The AA 1050 alloy was supplied as cold rolled plates of 15 mm thickness. The sea water was obtained from the eastern region (Jubail, Dammam, Saudi Arabia) of the Arabian Gulf and was used as received. An electrochemical cell with a three-electrode configuration was used for electrochemical measurements. The AA 1050 rod, a platinum foil, and a Metrohm Ag/AgCl electrode (in 3.0 M KCl)

were used as working, counter, and reference electrodes, respectively. The AA 1050 rods for electrochemical measurements were prepared by soldering a copper wire to one face of the rod; the rod with the attached wire were then cold mounted in resin and left to dry in air for 24 h at room temperature. Before measurements, the other face of the Al electrode was ground successively with metallographic emery paper of increasing fineness up to 800 grits, in accordance with standard procedures. The surfaces were then washed with doubly distilled water, degreased with acetone, washed using doubly distilled water again and finally dried with tissue paper. In order to prevent the possibility of crevice corrosion during measurement, the interface between sample and resin was coated with Bostik Quickset, a polyacrelate resin. The total exposed surface area of the working electrode was 1.0 cm^2.

2.2. Processing of the ECAPed AA 1050

ECAPed AA 1050 alloys were fabricated by using a special die [24], whose schematic diagram has been reported in our previous work [3]. The die was made from hot-work tool steel and consists of two channels equal in cross section, intersecting at an angle ϕ of 90^o [3, 24] . There is also an additional angle Ψ, which defines the arc of curvature at the outer point of intersection of the two channels. The value of angle Ψ was 0^o.

Cylindrical samples of AA 1050 were machined parallel to the rolling direction, and then annealed at a temperature of 600 ^oC for 8 hours, to give an average grain size of about 600 μm. The annealed samples were lubricated using graphite based lubricant and pressed in the ECAP die. Route B_C, where the sample was rotated by 90^o between subsequent pressings was adopted in the present study [24, 36]. Samples were processed to 4, 6, 8, 12 and 16 passes of route B_C. This route was shown to produce the finest substructure [33].

2.3. Electrochemical corrosion techniques

Corrosion tests were carried out by using an Autolab Potentiostat (PGSTAT20 computer controlled) operated by the general purpose electrochemical software (GPES) version 4.9. The cyclic potentiodynamic polarization curves were obtained by scanning the potential in the forward direction from -1800 to -500 mV against Ag/AgCl at a scan rate of 3.0mV/s; the potential was then reversed in the backward direction. Chronoamperometric current-time experiments were obtained by stepping the potential of the AA 1050 rods at – 630 mV versus Ag/AgCl; in some experiments this potential value was applied after stepping the potential of Al to – 1000 mV vs. Ag/AgCl for 20 min. Electrochemical impedance spectroscopy data were recorded for the alloys at corrosion potentials (E_{Corr}) after 20 min immersion in the test solution. The frequency was scanned from 100000 Hz to 0.1 Hz, with an ac wave of ± 5 mV peak-to-peak overlaid on a dc bias potential, and the impedance data were collected using Powersine software at a rate of 10 points per decade change in frequency. ZSimpWin software was used to fit the impedance data to best equivalent circuit for Al rods in AGS. All the electrochemical

experiments were recorded after immersion of the electrode in the test solution for 20 min and in some cases the electrodes were immersed for 10 days before measurements.

3. RESULTS AND DISCUSSION

3.1. Cyclic potentiodynamic polarization measurements

Cyclic potentiodynamic polarization (CPP) curves obtained for (a) 0 pass, (b) 4 passes, (c) 6 passes, (d) 8 passes, (e) 12 passes, and (f) 16 passes ECAPed AA 1050 electrode, respectively after 20 minutes immersion in AGS are shown in Fig. 1. The effect of ECAP process on the corrosion behavior of AA 1050 after (a) 0, (b) 4, and (c) 16 pass times was also performed after 10 days immersion in AGS and the curves are shown respectively in Fig. 2.

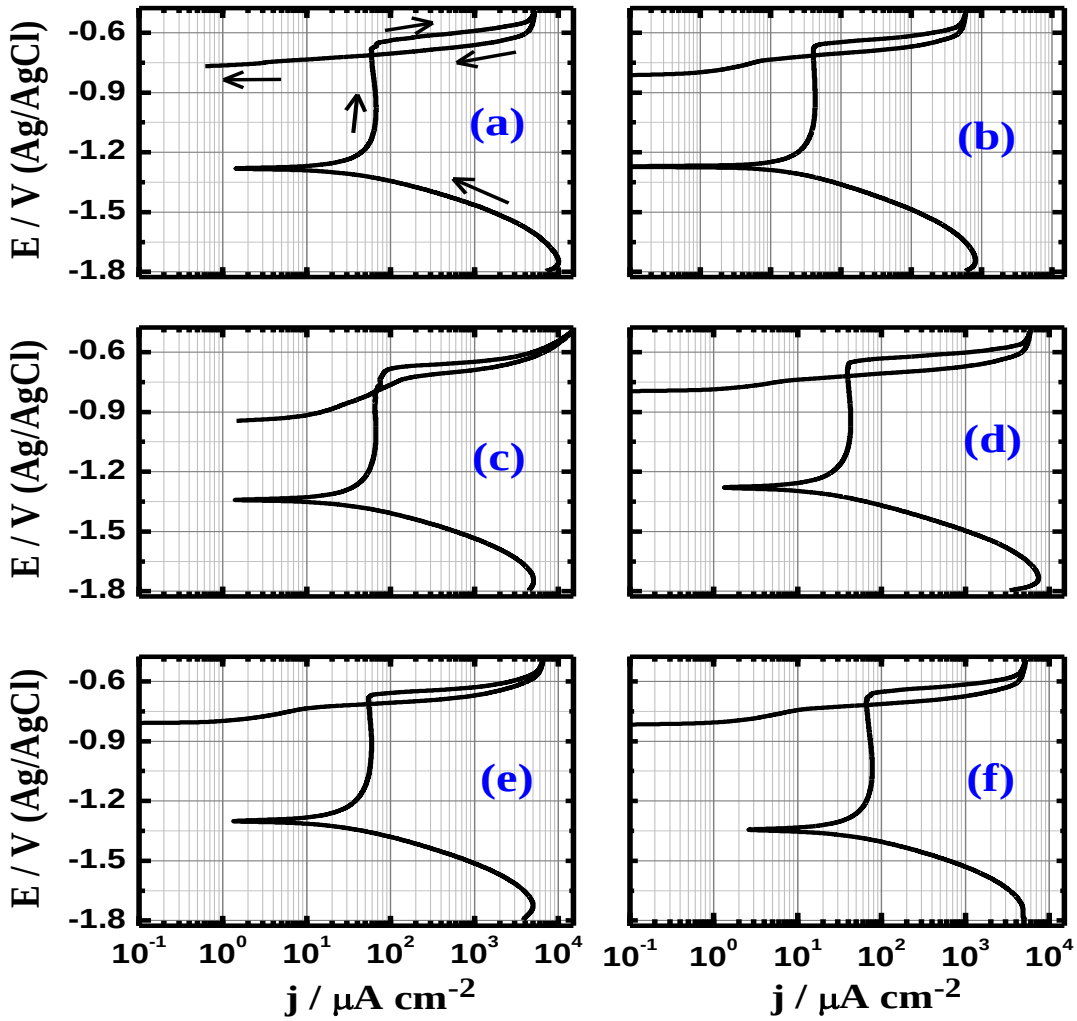

Figure 1. Cyclic potentiodynamic polarization curves obtained for (a) 0 pass, (b) 4 passes, (c) 6 passes, (d) 8 passes, (e) 12 passes, and (f) 16 passes ECAPed AA 1050 electrode, respectively after its immersion in AGS for 20 minutes.

The CPP measurements were carried out to report the effect of increasing ECAP pass time number, from 0 to 16, on the corrosion parameters of the AA 1050 after its immersion in open to air AGS solutions for 20 min and 10 days at room temperature. The values of corrosion potential (E_{Corr}), cathodic (βc) and anodic Tafel slopes (βa), corrosion current (j_{Corr}), passivation current (j_{Pass}), protection potential (E_{Prot}), pitting potential (E_{Pit}), polarization resistance (R_P), and corrosion rate (K_{Corr}), obtained from Fig. 1 and Fig. 2 are listed in Table 1. The values of these corrosion obtained from the polarization data as reported in our previous study [37-41].

The anodic reaction of Al that is shown in Fig. 1 (a) starts from a potential value of –1285 mV vs. Ag/AgCl towards the less negative potential values. It is clearly seen that Al shows a passive region at an average current density of ~ 62μA/cm^2, extending from −1150 to −680 mV due to the formation of an aluminum oxide on its surface [1-4];

$$2Al_{(S)} + 6OH^- = Al_2O_3.3H_2O + 6e^- \quad (1)$$

Aluminum oxide at this condition consists of an adherent, compact, and stable inner oxide film covered with a porous and less stable outer layer.

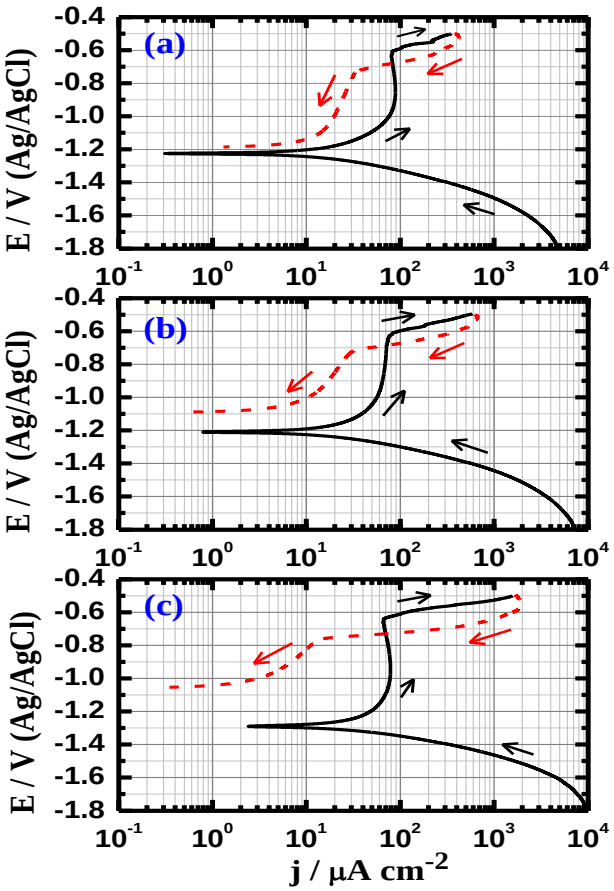

Figure 2. Cyclic potentiodynamic polarization curves obtained for (a) 0 pass, (b) 4 passes, and (c) 16 passes ECAPed AA 1050 electrode, respectively after immersion of samples in AGS for 10 days.

This dual nature of the oxide film allows aluminum to be more susceptible to corrosion [22,32,33]. This oxide was formed due to the transformation of an oxide that was also formed on aluminum surface according to the following equation [13];

$$Al_{(S)} + 3OH^- = Al(OH)_{3,ads.} + 3e^- \quad (2)$$

Increasing the applied potential increases the values of current as a result of the dissolution of the formed oxide film accompanied by the occurrence of pitting corrosion and eventually leads to the dissolution of aluminum as follows [10-13];

$$Al = Al^{3+} + 3e^- \quad (3)$$

Here, the occurrence of pitting corrosion was also indicated by the appearance of the hysteresis loop on reversing the potential scan in the backward direction towards the more negative values. The appearance of such loop was indicated by increasing the current values in the backward direction compared to those values recorded in the forward scan.

Table 1. Corrosion parameters obtained from polarization curves shown in Fig. 1 and Fig. 2 for the ECAPed AA 1050 electrodes after 20 min immersion in the Arabian Gulf seawater.

AA 1050 alloy	Parameter								
	$-B_c$ / mV dec^{-1}	E_{Corr} / mV	j_{Corr} / μA cm^{-2}	B_a / mV dec^{-1}	j_{Pass} / μA cm^{-2}	E_{Prot} / mV	E_{Pit} / mV	R_p / Ω cm^2	K_{Corr}/ mmy^{-1}
0 pass (20 min)	100	-1285	27	110	62.2	-720	-655	0.84	0.098
4 pass (20 min)	110	-1255	15	125	42.1	-710	-640	1.70	0.054
6 pass (20 min)	110	-1260	16	127	49.9	-705	-643	1.60	0.058
8 pass (20 min)	113	-1260	18	130	41.9	-720	-650	1.46	0.065
12 pass (20 min)	120	-1290	20	145	56.8	-720	-665	1.43	0.073
16 pass (20 min)	120	-1330	23	155	73.4	-725	-665	1.28	0.084
0 pass (10 day)	135	-1225	19	153	89.7	-680	-610	1.64	0.069
4 pass (10 day)	140	-1210	13	155	61.6	-680	-620	2.46	0.047
16 pass (10 day)	143	-1285	17	158	77.5	-735	-630	1.92	0.062

It has been reported [3] that the released aluminum cations, Al^{3+}, react with chloride ions present in seawater to form the soluble aluminum chloride complex, $AlCl_4^-$, according to the following reaction;

$$Al^{3+} + 4Cl^- = AlCl_4^- \quad (4)$$

According to Hunkeler et al. [42], pitting corrosion occurs at these conditions due to the formation of a salt barrier of $AlCl_3$ within the pits on their formation. This barrier leads to the formation of $AlCl_4^-$, reaction (4), which diffuses into the bulk of the solution leaving the aluminum surface pitted. On the other hand, Tomcsanyi et al. [43] have reported that Al suffers pitting corrosion due to the chemical adsorption of the existed chloride ions in the solution onto the aluminum oxide surface to act as a reaction partner and aiding the oxide to dissolve via the formation of oxychloride complexes as follows;

$$Al^{3+}_{\text{(in crystal lattice of the oxide)}} + 2Cl^- + 2OH^- = Al(OH)_2Cl_2^- \qquad (5)$$

The cathodic reaction that consumes the electron produced by the anodic dissolution of Al in the corrosive near neutral aerated solutions has been reported to the oxygen reduction as can be represented by the equation [44-47];

$$O_2 + 2H_2O + 4e^- = 4OH^- \qquad (6)$$

The polarization curves for the ECAPed AA 1050 after 4 passes, Fig. 1b shows almost similar behavior except that the values of j_{Corr}, j_{Pass}, and K_{Corr} were very less and the value of R_P is increased. Increasing the number of passes thereafter, i.e. 6, 8, 12 and 16 increased the values of j_{Corr}, j_{Pass}, and K_{Corr} compared to their values after 4 passes but still lower than the corresponding values for the annealed Al as shown in Fig. 1a. This means that the ECAPed Al after 4 passes shows the best performance against corrosion in AGS solution. The corrosion resistance of ECAPed Al recorded the highest at 4 passes and started to decrease with increasing the number of passes up to 16. This was also confirmed by the CPP curves of Fig. 2 and corrosion parameters listed in Table 1 for AA 1050 after 10 days immersion in AGS solutions. In all cases, the ECAPed alloys showed lower corrosion rate and higher corrosion resistance compared to the annealed one. Under these conditions, the increase of ECAP pass number increases the corrosion resistance of AA 1050 due to the decreasing of the size of the Si-containing impurities on the alloy surface [48]. Where, the presence of these Si-containing impurities induced the micro-galvanic reaction by its reaction with the Al matrix and also between the Al matrix and the Si-containing oxide. The decrease of corrosion resistance for the number of passes more than 4 may be attributed to increase of severity of plastic deformation and increasing the dislocation density.

3.2. Chronoamperometric current-time measurements

Chronoamperometric current-time (CT) curves obtained for 0 pass (1), 4 passes (2), 6 passes (3), 8 passes (4), 12 passes (5), and 16 passes (6) AA 1050 electrode, respectively, after its immersion in AGS for 20 minutes followed by stepping the potential to –0.63 V vs. Ag/AgCl are shown in Fig. 3. The CT method have been frequently employed in studying the effect of changing inhibitor concentration [49-51], metallic additive [38,52,53], nanofiber coatings [54] and corrosive environment

[46,55] at constant anodic potential on the corrosion of metals and alloys. The currents obtained for the annealed Al, Fig. 3, curve 1, recorded the highest current values in the first 10 min due to the corrosivity of the seawater and the occurrence of pitting corrosion. The current then started to decrease slightly with time till the end of the run, which was probably resulted from the repassivation of the formed pits [3]. On the hand, the current values showed its minimum for the 4 passes AA 1050 alloy, Fig. 3, curve 2, which indicates that both pitting and uniform corrosion were reduced. Increasing the number of passes to 6, 8, 12 and 16 gradually increased the recorded current with time, which is in good agreement with the data obtained from polarization measurements.

In order to confirm the effect of number of passes on the variation of current values with time after long immersion time, the CT curves at –0.63 V vs. Ag/AgCl were obtained for AA 1050 after 0 pass (1), 4 passes (2), 8 passes (3), and 16 passes (4), respectively after 10 days immersion in AGS and the data are shown in Fig. 4.

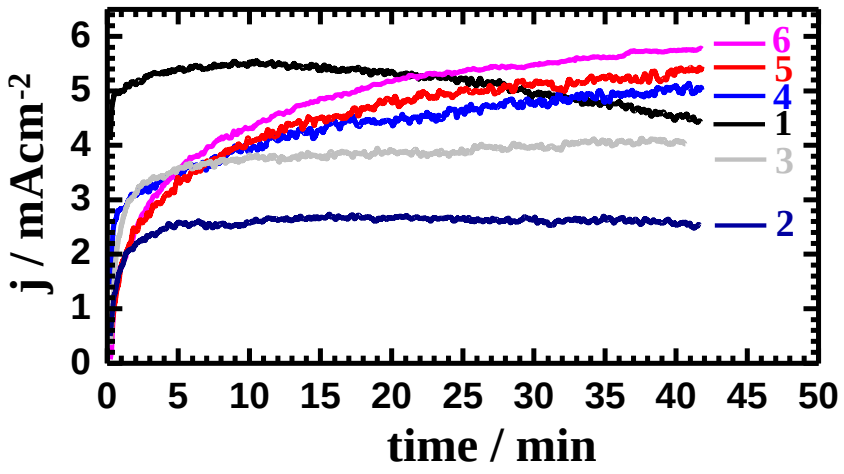

Figure 3. Chronoamperometric curves obtained for (1) 0 pass, (2) 4 passes, (3) 6 passes, (4) 8 passes, (5) 12 passes, and (6) 16 passes ECAPed AA 1050 electrode, respectively after its immersion in AGS for 20 minutes followed by stepping the potential to –0.63 V vs. Ag/AgCl.

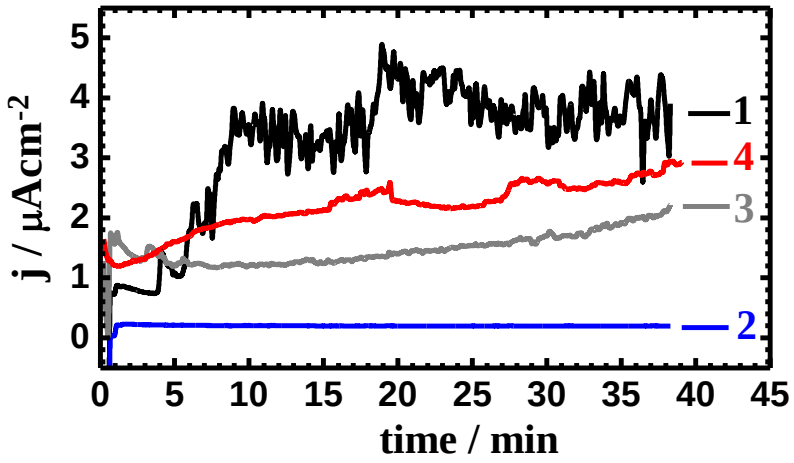

Figure 4. Chronoamperometric curves obtained for (1) 0 pass, (2) 4 passes, (3) 8 passes and (4) 16 passes ECAPed AA 1050 rods after their immersion in AGS for 10 days before stepping the potential to –0.63 V vs. Ag/AgCl.

It is clearly seen from Fig. 4 that the annealed Al alloy (0 pass) shows the highest current values accompanied with large fluctuations that increase with increasing time. It is also seen that Al alloy subjected to 4 passes, recorded the lowest current values with no fluctuations and the current is constant with time. Increasing the number of passes to 8 and further to 16, increased the current compared to that obtained with 4 passes but still lower than that for the annealed alloy (0 pass). This agrees with the CT data obtained after 20 min and confirms that the ECAPed alloy obtained after 4 passes had the highest corrosion resistance.

The CT curves obtained for various ECAPed AA 1050 electrode after its immersion in AGS for 10 min at -1.0 V before stepping the potential to –0.63 V vs. Ag/AgCl are shown in Fig. 5. These experiments were carried out in order to study the effect of the number of passes on the pitting corrosion of Al after developing a passive film on its surface by applying a constant potential of –1.0 V, which was chosen from the CPP curves for 10 min before increasing the potential to an active anodic potential value, –0.63 V. It is clear from Fig. 5 that the current values recorded only few microamperes for all alloys when the potential was set to the passive value, –1.0 V, due probably to the formation of aluminum oxide layers on the surface of the alloys [3,10]. Shifting the potential to the active value, –0.63 V, increases the output current values particularly in the first few min of potential application. It is also seen that the current recorded the highest values in the active potential for the annealed alloy, which confirms that that alloy had the worst corrosion resistance. On the other hand, the lowest currents were obtained for the ECAPed alloy after 4 passes, which also confirms that this alloy had the highest corrosion resistance. Increasing pass number to 6, 8, 12 and 16 lead to an increase in the obtained current higher than that for 4 passes ECAPed Al.

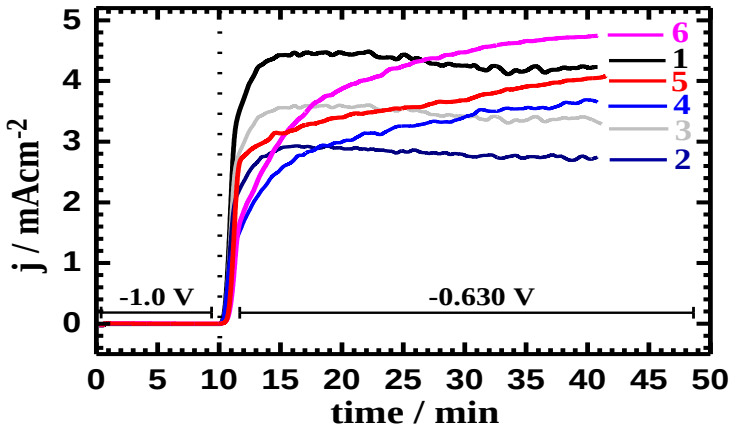

Figure 5. Chronoamperometric curves obtained for (1) 0 pass, (2) 4 passes, (3) 6 passes, (4) 8 passes, (5) 12 passes, and (6) 16 passes ECAPed AA 1050 electrode after its immersion in AGS for 10 min at -1.0 V before stepping the potential to –0.63 V for 32 min (all potentials were vs. Ag/AgCl).

3.3. Electrochemical impedance spectroscopy measurements

In order to determine the kinetic parameters for electron transfer reactions at the Al/AGS interface, electrochemical impedance spectroscopy (EIS) measurements were carried out. Typical

Nyquist plots obtained for ECAPed AA 1050 electrode at an open circuit potential after its immersion in AGS for 20 min are shown in Fig. 6. The EIS data were also recorded after 10 days immersion in AGS solution in order to study the effect of pass number on the corrosion behavior of Al alloy. Figure 7 shows the Nyquist (a), Bode (b) and phase angle (c) plots for (1) 0 pass, (2) 4 passes and (3) 16 passes ECAPed AA 1050 electrode at an open circuit potential after its immersion in AGS for 10 days. The Nyquist plots shown in Fig. 6 and Fig. 7a were analysed by fitting to the equivalent circuit model shown in Fig. 8. The impedance parameters obtained by fitting the equivalent circuit of Fig. 8 are listed in Table 2.

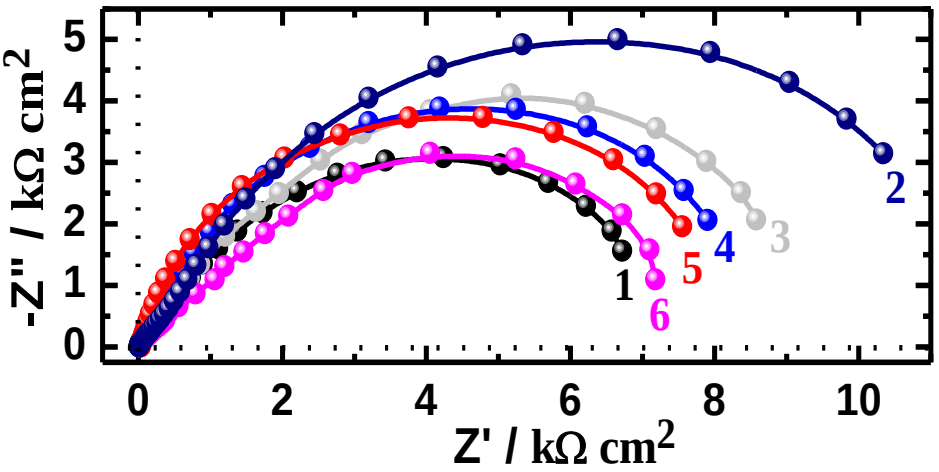

Figure 6. Nyquist plots obtained for (1) 0 pass, (2) 4 passes, (3) 6 passes, (4) 8 passes, (5) 12 passes, and (6) 16 passes ECAPed AA 1050 electrode at an open circuit potential after its immersion in AGS for 20 min.

According to usual convention, the parameters of the circuit shown in Fig. 8 can be defined as follows; R_S represents the solution resistance between Al surface and the platinum counter electrode; Q the constant phase elements (CPEs) and contain two parameters; a pseudo capacitance and an exponent (n), which is less than unity and indicates a dispersion of capacitor effects [10-13]; R_{P1} accounts for the resistance of a film layer formed on the surface of Al alloy; C_{dl} is the double layer capacitance; and R_{P2} represents the charge transfer resistance and account for the polarization resistance of the Al surface.

It is clearly seen from Fig. 6 that all alloys show one semicircle and the lowest diameter of them is for the 0 pass time Al alloy, Fig. 6, curve 1. On the other hand, the highest width of the diameters was recorded for AA 1050 after 4 passes as represented by curve 2 of Fig. 6. Increasing pass time number to 6, curve 3, shows a little decrease in the diameter and this effect increases with increasing the ECAP pass time to 8, 12, and 16. This indicates that the best performance amongst Al alloys was produced by AA 1050 processed 4 passes. The same behavior was also obtained for Al alloys after its immersion for 10 days in AGS as can be seen from Fig. 7a. The 10 days immersion time allowed the diameter of the semicircles for all alloys to increase compared to 20 min measurements. This is because the long immersion time helps Al to develop a layer of corrosion products that partially protect the surface against corrosion and thus increase the corrosion resistance. Nyquist spectra shown

in Fig. 6 and Fig. 7a with the parameters recorded in Table 2 clearly revealed that the values of R_S, R_{P1} and R_{P2} increased with increasing the pass time number for the AA 1050 alloy. The values of R_{P1} and R_{P2} are a measure of the uniform corrosion rate, which decreases very much with increasing immersion time as indicated by the high values of these resistances for the 10 days experiments.

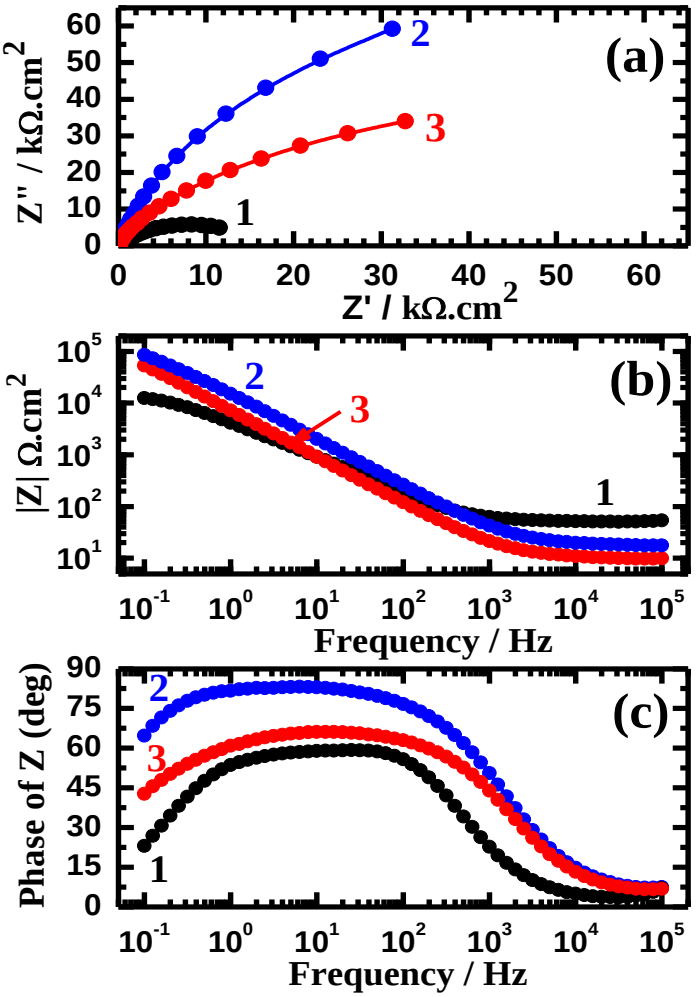

Figure 7. Nyquist (a), Bode (b) and phase angle (c) plots for (1) 0 pass, (2) 4 passes and (3) 16 passes ECAPed AA 1050 electrode after its immersion in AGS for 10 days.

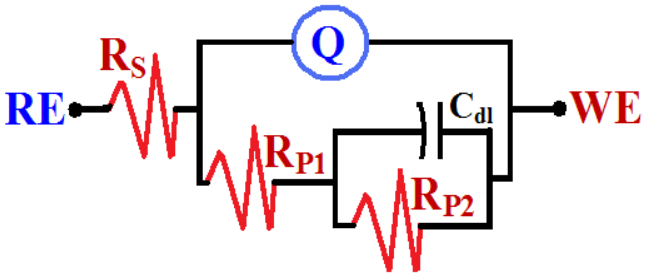

Figure 8. The equivalent circuit model used to fit the EIS experimental data.

Table 2. EIS parameters obtained by fitting the Nyquist plots shown in Fig. 6 and Fig. 7a with the equivalent circuit shown in Fig. 8 for AA 1050 electrodes after 20 min and 10 days of immersion in Arabian Gulf water.

AA 1050 alloy	Parameter					
	R_S / Ω cm^2	Q		R_{P1} / k Ω cm^2	C_{dl} / μF cm^{-2}	R_{P2} / k Ω cm^2
		Y_Q/ μF cm^{-2}	n			
0 pass (20 min)	6.23	32.89	0.83	0.201	26.14	5.51
4 passes (20 min)	11.28	5.48	0.76	1.731	13.07	11.39
6 passes (20 min)	10.47	8.52	0.80	0.965	23.94	7.76
8 passes (20 min)	9.61	13.18	0.90	0.708	16.69	7.72
12 passes (20 min)	7.88	14.03	0.90	0.586	17.75	6.95
16 passes (20 min)	7.13	14.89	0.87	0.354	18.98	6.09
0 pass (10 days)	8.90	0.56	0.80	1.91	2.79	9.58
4 passes (10 days)	12.49	0.19	0.88	3.28	1.89	23.98
16 passes (10 days)	9.27	0.42	0.91	2.03	2.31	13.62

The CPEs (Q) with their n values < 1.0 represent double layer capacitors with some pores; the decrease of CPEs with the changing the number of ECAP passes and increasing immersion time confirm that the surface of Al gets more protection with varying the ECAP passes and increasing time. The values of C_{dl} decreased with ECAP pass number as well as the immersion time because of decreasing the dissolution of Al alloys via mass transport. The obtained data by Nyquist curves and EIS parameters shown in Table 2 were also confirmed by plotting the impedance of the interface and phase angle as shown in Fig. 7b and Fig. 7c, respectively. It is clearly seen that the impedance of the interface and the maximum phase angle increased with increasing the immersion time and ECAP pass to 4 times then its decreasing to 16. The EIS measurements thus are in good agreement with the polarization and Chronoamperometric data that Al alloys fabricated by ECAP process produce more corrosion resistance in the AGS solution. Also, elongating the immersion time of the alloy in AGS before measurements decreases its uniform corrosion.

4. CONCLUSIONS

The effect of ECAP process after 0, 4, 6, ,8,12, and 16 pass number on the corrosion behavior of AA 1050 aluminum alloy in natural aerated stagnant Arabian Gulf seawater after 20 min and 10 days was reported. The study was carried out using the conventional electrochemical methods such as cyclic potentiodynamic polarization and chronoamperometric current-time at constant potential along with the electrochemical impedance spectroscopy. Results indicated that annealed AA 1050 (0 passes) suffers both uniform and pitting corrosion after 20 min immersion in the AGS solution. ECAPed alloys showed lower corrosion and absolute current densities and corrosion rate and higher polarization and corrosion resistances. The ECAPed Al alloy after 4 passes time number recorded the lowest corrosion current and corrosion rate and highest corrosion resistance. Further increasing the ECAP pass number

increased the corrosion parameters compared to the alloy that was produced after 4 passes. The order of the best performance showed by the ECAPed AA 1050 against corrosion was obtained according to this order, 4 > 6 > 8 > 12 > 16 > 0 passes. Increasing the immersion time from 10 min to 10 days before measurement greatly decreased the corrosion of all studied AA 1050 alloys.

ACKNOWLEDGEMENT
This project was supported by King Saud University, Deanship of Scientific Research, College of Engineering Research Center.

References

1. El-Sayed M. Sherif, A. A. Almajid, F. H. Latif, H. Junaedi, *Int. J. Electrochem. Sci.,* 6 (2011) 1085.
2. F. H. Latief, El-Sayed M. Sherif, A. A. Almajid, H. Junaedi, *J. Anal. Appl. Pyrolysis,* 92 (2011) 485.
3. El-Sayed M. Sherif, E. A. El-Danaf, M.S. Soliman, A. A. Almajid, *Int. J. Electrochem. Sci.,* 7 (2012) 2846.
4. El-Sayed M. Sherif, F. H. Latif, H. Junaedi, A. A. Almajid, *Int. J. Electrochem. Sci.,* 7 (2012) 4352.
5. W. Diggle, T. C. Downie, C. Goulding, *Electrochim. Acta,* 15 (1970) 1079.
6. F. H. Latief, El-Sayed M. Sherif, *J. Ind. Eng. Chem.,* 18 (2012) 2129.
7. G. A. Capauano, W. G. Davenport, *J. Electrochem. Soc.,* 118 (1971) 1688.
8. P. Fellener, M. C. Paucivova, K. Mataisovsky, *Surf. Coat. Technol.,* 14 (1981) 101.
9. A. A. El-Shafei, S. A. Abd El-Maksoud, A. S. Fouda, *Corros. Sci.,* 46 (2004) 579.
10. El-Sayed M. Sherif, *Int. J. Electrochem. Sci.,* 7 (2012) 4847.
11. El-Sayed M. Sherif, *Int. J. Electrochem. Sci.,* 6 (2011) 1479.
12. E. M. Sherif, S.-M. Park, *Electrochim. Acta*, 51 (2006) 1313.
13. E. M. Sherif, S.-M. Park, *J. Electrochem. Soc.,* 152 (2005) B205.
14. N. A. Ogurtsov, A. A. Pud, P. Kamarchik, G.S. Shapoval, *Synth. Met.,* 143 (2004) 43.
15. I. B. Obot1, N. O. Obi-Egbedi, *Int. J. Electrochem. Sci.,* 4 (2009) 1277.
16. A. Y. El-Etre, *Corros. Sci*., 43 (2001) 1031.
17. S. B. Saidman, J. B. Bessone, *J. Electroanal. Chem.,* 521 (2002) 87.
18. P. M. Natishan, E. McCafferty, G. K. Hubler, *J. Electrochem. Soc.,* 135 (1988) 321.
19. C. M. A. Brett, I. A. R. Gomes, J. P. S. Martins, *Corros. Sci.,* 36 (1994) 915.
20. S. S. A. Rehim, H. H. Hassan, M.A. Amin, *Appl. Surf. Sci.,* 187 (2002) 279.
21. S. Zein El Abedin, *J. Appl. Electrochem.,* 31 (2001) 711.
22. J.M. Vega, N. Granizo, D. de la Fuente, J. Simancas, M. Morcillo, Prog. Org. Coat. 70 (2011) 213.
23. R. Zandi-zand, A. Ershad-langroudi, A. Rahimi, *J. Non-Crystalline Solids,* 351 (2005) 1307.
24. E. A. El-Danaf, M. S. Soliman, A. A. Almajid, M. M. El-Rayes, *Mater. Sci. Eng. A,* 458 (2007) 226.
25. Cheng Xu, S. V. Dobatkin, Z. Horita, T. G. Langdon, *Mater. Sci. Eng. A,* 500 (2009) 170.
26. Ehab A. El-Danaf, *Mater. Sci. Eng. A,* 487 (2008) 189.
27. M. Furukawa, Z. Horita, M. Nemoto, T.G. Langdon, *J. Mater. Sci*. 36 (2001) 2835.
28. Eiji Akiyama, Zuogui Zhang, Yoshimi Watanabe, Kaneaki Tsuzaki, *J. Solid State Electrochem.,* 13 (2009) 277.
29. M. Fujda, T. Kvačkaj, K. Nagyová, *J. Met. Mater. Miner.,* 18 (2008) 81.

30. J.-H. Jiang, A.-B. Ma, F.-M. Lu, N. Saito, A. Watazu, D. Song, P. Zhang and Y. Nishida, *Mater. Corros.,* 62 (2011) 848.
31. M. Furukawa, Z. Horita, T. G. Langdon, *Adv. Eng. Mater.,* 3 (2001) 121.
32. Z. Horita, S. Lee, S. Ota, K. Neishi, T.G. Langdon, *Mater. Sci. Forum.* 357–359 (2001) 471.
33. R.Z. Valiev, T.G. Langdon, *Prog. Mater. Sci.,* 51 (2006) 881.
34. Dan Song, AiBin Ma, Jinghua Jiang, Pinghua Lin, Donghui Yang, Junfeng Fan, *Corros. Sci.,* 52 (2010) 481.
35. A. Vinogradov, A. Washikita, K. Kitagawa, V. I. Kopylov, *Mater. Sci. Eng. A,* 349 (2003) 218.
36. Zhang Jing, Zhang Ke-shi, Wu Hwai-Chung, YU Mei-hua, *Trans. Nonferrous Met. Soc. China,* 19 (2009) 1303.
37. El-Sayed M. Sherif, A. A. Almajid, *J. Appl. Electrochem.*, 40 (2010) 1555.
38. El-Sayed M. Sherif, J. H. Potgieter, J. D. Comins, L. Cornish, P. A. Olubambi, C. N. Machio, *J. Appl. Electrochem.,* 39 (2009) 1385.
39. El-Sayed M. Sherif, *J. Mater. Eng. Perform.*, 19 (2010) 873.
40. El-Sayed M. Sherif, A. Y. Ahmed, *Synthesis and Reactivity in Inorganic, Metal-Organic, and Nano-Metal Chemistry,* 40 (2010) 365.
41. El-Sayed M. Sherif, A.A. Almajid, *Int. J. Electrochem. Sci.,* 6 (2011) 2131.
42. F. Hunkeler, G. S. Frankel, H. Bohni, *Corrosion (Houston),* 43 (1987) 189.
43. L. Tomcsanyi, K. Varga, I. Bartik, G. Horanyi, E. Maleczki, *Electrochim. Acta,* 34 (1989) 855.
44. El-Sayed M. Sherif, *Mater. Chem. Phys.,* 129 (2011) 961.
45. El-Sayed M. Sherif, *Int. J. Electrochem. Sci.,* 6 (2011) 3077.
46. El-Sayed M. Sherif, A. A. Almajid, A. K. Bairamov, Eissa Al-Zahrani, *Int. J. Electrochem. Sci.,* 6 (2011) 5430.
47. El-Sayed M. Sherif, *J. Solid State Electrochem.,* 16 (2012) 891.
48. Min-Kyong Chung, Yoon-Seok Choi, Jung-Gu Kim, Young-Man Kim, Jae-Chul Lee, *Mater. Sci. Eng*. A, 366 (2004) 282.
49. El-Sayed M. Sherif, *Int. J. Electrochem. Sci*., 7 (2012) 4235.
50. El-Sayed M. Sherif, *Int. J. Electrochem. Sci*., 7 (2012) 4834.
51. El-Sayed M. Sherif, *Int. J. Electrochem. Sci*., 7 (2012) 5084.
52. El-Sayed M. Sherif, J. H. Potgieter, J. D. Comins, L. Cornish, P. A. Olubambi, C. N. Machio, *Corros. Sci.,* 51 (2009) 1364.
53. J. H. Potgieter, P. A. Olubambi, L. Cornish, C. N. Machio, El-Sayed M. Sherif, *Corros. Sci.,* 50 (2008) 2572.
54. El-Sayed M. Sherif, Mahir Es-saheb, Ahmed A. Elzatahry, El-Refaie kenawy, Ahmad S. Alkaraki, *Int. J. Electrochem. Sci.,* 7 (2012) 6154.
55. El-Sayed M. Sherif, A.A. Almajid, A.K. Bairamov, Eissa Al-Zahrani, *Int. J. Electrochem. Sci.,* 7 (2012) 2796.